Available online at www.sciencedirect.com

ScienceDirect

Palaeoworld

Palaeoworld 28 (2019) 37–50

www.elsevier.com/locate/palwor

Review

# Links between early Paleozoic oxygenation and the Great Ordovician Biodiversification Event (GOBE): A review

Cole T. Edwards

*Department of Geological and Environmental Sciences, Appalachian State University, Boone, NC 28608, USA*

Received 6 March 2018; received in revised form 27 July 2018; accepted 23 August 2018
Available online 30 August 2018

**Abstract**

The Great Ordovician Biodiversification Event (GOBE) represents a four-fold increase of genus-level diversity that post-dates the diversification of the 'Cambrian explosion' by 40–50 Myr. A major increase in atmospheric oxygen ($O_2$) levels is thought to be a leading cause of the 'Cambrian explosion' that lowered metabolic costs associated with skeletal and collagen biomineralization. The cause(s) of the GOBE, however, is (are) less well understood, and may include a cooling climate, increased nutrient availability, higher sea levels and increased ecospace, and further oxygenation of shallow marine environments. Atmospheric $O_2$ levels are difficult to quantitatively estimate, particularly whether oxygenation was a plausible driver of the GOBE, because $O_2$ estimates are hampered in part by the coarse time resolution of redox proxy records (e.g., iron-based geochemical data) and isotope mass balance models. Newly published high-resolution geochemical trends are used to better constrain the timing and degree of oxygenation across the GOBE, which include traditional methods such as stable carbon ($\delta^{13}C$) and sulfur ($\delta^{34}S$) isotope trends to estimate $O_2$ levels on a global scale, and local-scale redox-sensitive proxies such as iodine (I/Ca) and trace metal concentrations and isotopes (e.g., Mo and U). Taken together, geochemical evidence suggests that Ordovician environments became progressively more oxygenated following the end of recurrent anoxic events and extinctions of late Cambrian and Early Ordovician marine faunas. A sluggishly circulating Cambrian global ocean could have maintained an oxycline in the water column that impinged upon the continental shelf, which extended into wide expanses of shallow shelf settings during relative sea level rises that caused positive $\delta^{13}C$ and $\delta^{34}S$ excursions and mass extinctions. Ordovician oxygenation roughly corresponds to cessation of positive $\delta^{13}C$ excursions (i.e., shallow water anoxia) and the major pulses of biodiversification that comprise the GOBE, suggesting that oxygenation was an important driver of Ordovician biodiversity. Anoxic conditions below an oxycline that impinged upon the continental shelf likely persisted until the Devonian when a cooler climate invigorated circulation and ventilated the global ocean, with the possible exception of some isolated basins that were persistently anoxic.
Published by Elsevier B.V. on behalf of Nanjing Institute of Geology and Palaeontology, CAS.

*Keywords:* Oxygenation; Ordovician; Biodiversity; Atmospheric modeling; Carbon isotopes; Carbonate-associated sulfate

## Contents



*E-mail address:* edwardsct4@appstate.edu

https://doi.org/10.1016/j.palwor.2018.08.006
1871-174X/Published by Elsevier B.V. on behalf of Nanjing Institute of Geology and Palaeontology, CAS.

## 1. Introduction

The origin and diversification of metazoan life is widely thought to be linked to the oxygenation of the ocean-atmosphere system, particularly with respect to the major radiation of metazoan life associated with Ediacaran–Cambrian transition (Butterfield, 2011; Mills et al., 2014; Chen et al., 2015) and the 'Cambrian explosion' (Nursall, 1959; Cloud, 1968; Knoll and Carroll, 1999; Berner et al., 2007; Sperling et al., 2015a). Oxygenation of the atmosphere and shallow ocean could expand habitable ecospace for animal life in an otherwise poorly oxygenated ocean, allow for larger body sizes as respiration efficiency increased (Raff and Raff, 1970), and eased energetic costs associated with biosynthesis of collagen and calcareous skeletal material (Towe, 1970; Pruss et al., 2010). Following a major increase of $O_2$ levels in shallow environments near the beginning of the Cambrian, based on iron-speciation data (Sperling et al., 2015b) — a local proxy for water column and pore water redox conditions — and possible predation pressure (Sperling et al., 2013, 2015a), oceans appear to have become progressively oxygenated throughout the early Paleozoic where near-modern atmospheric $O_2$ levels may have been reached several times, including the late Cambrian (Saltzman et al., 2011) and Middle–Late Ordovician (Berner et al., 2007; Edwards et al., 2017). High atmospheric $O_2$ levels and an oxygenated ocean was finally maintained by the Devonian (Dahl et al., 2010; Lenton et al., 2016, 2018), likely due to the successful establishment of land plants (Wallace et al., 2017). Quantitative estimates of atmospheric $O_2$ levels, however, are fraught with assumptions that require well-preserved and appropriate geochemical proxy records to inform atmospheric $O_2$ models.

Agreement between geochemical-based models with independent redox-sensitive proxies increases confidence in $O_2$ estimates, but these estimates require that the applied geochemical signature faithfully captures a global signal, which may not be possible for some proxies (e.g., iron speciation and at times trace metal concentrations). Paleozoic carbon isotopic trends ($\delta^{13}C$) are widely used to estimate organic carbon burial rates that affect ancient $O_2$ levels and are measured primarily from shelf settings thought to capture a global signal (Bachan et al., 2017). This may also be true for other geochemical proxy data measured from carbonates that formed in shallow shelf settings (e.g., carbonate-associated sulfate: CAS). This notion that platform carbonates can preserve a global signal has been questioned (e.g., Swart and Eberli, 2005; Swart, 2008) based on discordant $\delta^{13}C$ trends from shelf-to-basin transects of carbonate sediment along the modern-day Bahamian platform. However, positive $\delta^{13}C$ excursions measured from Cretaceous black shale lithologies recovered from the deep-ocean are in good agreement to age-equivalent shallow-water carbonate and black shale facies (Erbacher et al., 2005; Lu et al., 2010; Owens et al., 2013, 2016, 2017; Dickson et al., 2016), indicating that it is possible to use $\delta^{13}C$ trends measured from shallow shelf carbonates to infer changes to the global carbon cycle and periods of elevated organic carbon burial under reducing conditions.

The early Paleozoic has been the focus of numerous studies over the past two decades where workgroups have documented several globally preserved geochemical perturbations, namely with respect to the carbon ($\delta^{13}C$) and sulfur ($\delta^{34}S$) records, as well as drawing inferences about their paleoenvironmental importance and impact to the biosphere (e.g., Saltzman et al., 1998, 2000, 2011, 2015; Buggisch et al., 2003; Cramer and Saltzman, 2005, 2007; Maloof et al., 2005, 2010; Saltzman and Young, 2005; Gill et al., 2007, 2011; Young et al., 2008, 2010, 2016; Bergström et al., 2010; Jones et al., 2011; Hammarlund et al., 2012; Thompson and Kah, 2012; Jones and Fike, 2013; Dahl et al., 2014; Edwards and Saltzman, 2014, 2016; Kah et al., 2016; Quinton et al., 2016; Schiffbauer et al., 2017; Edwards et al., 2018). Some of these studies also use isotope-mass balance modeling to explore how the expansion and duration of reducing waters (anoxic to euxinic) could produce the observed positive $\delta^{13}C$ and $\delta^{34}S$ excursions (Gill et al., 2011; Saltzman et al., 2011; Jones and Fike, 2013; Young et al., 2016). These recurrent anoxic/euxinic events are sometimes linked to Cambrian–Ordovician extinctions of local faunas (Fig. 1; Saltzman et al., 2000, 2015; Edwards et al., 2018), but they are short-lived (<1–2 Myr), possibly due in part to the negative feedback associated with oxygen release from increased organic burial rates or a contraction of anoxic waters due to a relative sea level fall. These bio-geochemical events diminish and appear to end by the end of the Early Ordovician, prior to when atmospheric $O_2$ levels are thought to increase. Edwards et al. (2017) estimate that a near doubling of atmospheric $O_2$ levels occurred throughout the Ordovician (from ~13% to 25% by the Late Ordovician), which have been interpreted to be an important driver of the three-fold increase of marine families known as the Great Ordovician Biodiversification Event (GOBE). The GOBE has been hypothesized to be driven by other causes that facilitated biodiversification, including cooling oceans (Trotter et al., 2008), an increase and diversification of phytoplankton (Servais et al., 2008, 2010), and changes in substrates and the expansion of carbonate hardgrounds (Wilson et al., 1992; Miller and Connolly, 2001). The diversification that is the GOBE reached a maximum by the Late Ordovician and was maintained for much of the Paleozoic, despite several mass extinctions (e.g., Sepkoski, 1998). For most of the early Paleozoic, however, the global ocean may not have been fully oxygenated until the Devonian (Dahl et al., 2010; Lenton et al., 2016, 2018), particularly if an oxycline persisted in the water column due to sluggish global circulation. Though the link between oxygenation and diversifi-

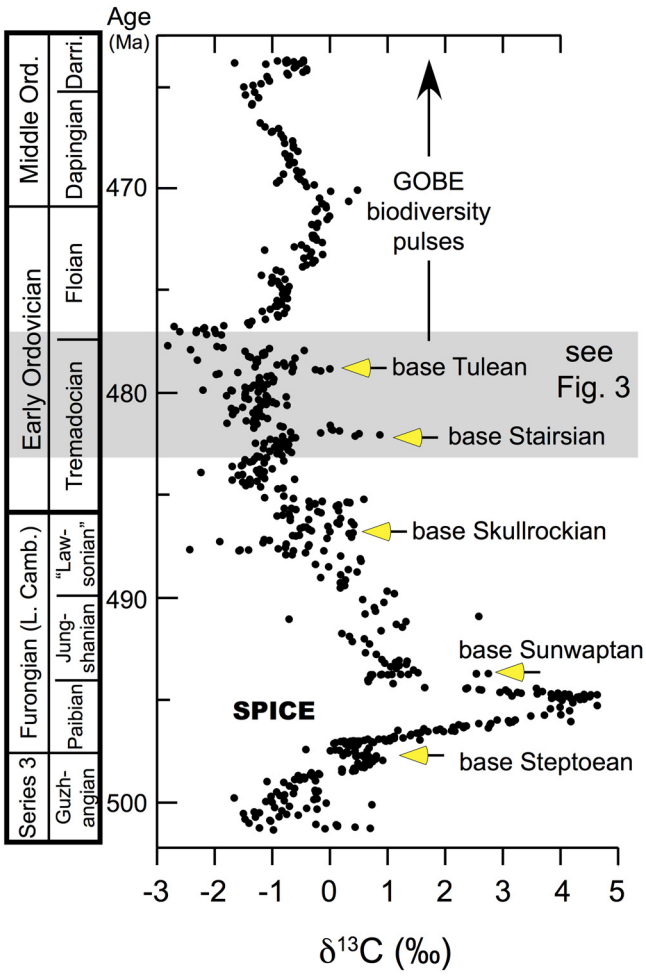


Fig. 1. $\delta^{13}C$ trend from the late Cambrian to Middle Ordovician with trilobite extinction events (yellow arrows). The late Cambrian SPICE event is the largest positive $\delta^{13}C$ excursion, followed by recurrent excursions that become less frequent with less positive maximum values, which end before the main biodiversity pulses that comprise the GOBE. Modified from Saltzman et al. (2015). Ord. = Ordovician, Darri. = Darriwilian, L. Camb. = Late Cambrian. (For interpretation of the references to color in this figure legend, the reader is referred to the web version of this article.)

cation is supported by the co-occurrence of the GOBE and rising $O_2$ levels, it remains unclear whether global $O_2$ levels directly regulate biodiversity over long periods of geologic time without better temporally resolved quantitative estimates.

## 2. Estimating oxygen levels: redox proxies and modeling

Quantitatively estimating $O_2$ levels in deep time is difficult, in part because reliable estimates must be made using well-preserved geochemical data that have been prevented from reacting with oxygen or other oxidizing agents since burial. Some studies use proxy data thought to track local redox conditions at the location of mineral precipitation in the water column and sediment profile during early diagenesis. Some of these proxies include I/Ca ratios of carbonate minerals (Lu et al., 2010; Zhou et al., 2015; Hardisty et al., 2017; Lu et al., 2018), iron speciation studies (Canfield et al., 1996; Poulton et al., 2004; Lyons and Severmann, 2006; Sperling et al., 2015b; Raiswell et al., 2018), molybdenum isotopes ($\delta^{97}Mo$ and $\delta^{98}Mo$; Arnold et al., 2004; Dahl et al., 2010; Dickson, 2017; Dickson et al., 2017) and concentrations (Anbar and Knoll, 2002; Algeo, 2004; Algeo and Lyons, 2006), and uranium isotopes ($\delta^{238}U$) and concentrations (Schovsbo, 2002; Weyer et al., 2008; Tissot and Dauphas, 2015; Elrick et al., 2017; Bartlett et al., 2018). Additional redox-sensitive trace metal concentrations of Zn, Mn, Pb, and V (Algeo, 2004), Cr isotopes and abundances (Frei et al., 2009; Reinhard et al., 2013), rare earth element patterns (Zhang et al., 2018), thallium (Tl) isotopes (Ostrander et al., 2017; Them et al., 2018), and Ce anomalies (Ling et al., 2013), but these proxies have mainly been applied to study the oxygen-poor Proterozoic ocean and Mesozoic Oceanic Anoxic Events and have yet to be as routinely applied to study early Paleozoic successions. [Though some of these proxies can differentiate between anoxic conditions that are sulfidic (e.g., iron speciation analysis) and non-sulfidic (e.g., I/Ca and Tl isotopes), for the purposes of this review the use of 'anoxic' or 'anoxia' herein refers to conditions with essentially no dissolved $O_2$ present, which can also include euxinic conditions where free $H_2S$ is present in the water column]. Other approaches use long-term $\delta^{13}C$ and $\delta^{34}S$ trends as a function of global organic carbon and pyrite burial rates, respectively, to indirectly estimate changes in atmospheric $O_2$ levels beyond whether oceans were either oxic or anoxic (Fig. 2; Berner et al., 2007; Royer et al., 2014; Lenton et al., 2016, 2018; Edwards et al., 2017). Though both approaches estimate $O_2$ levels at different scales (local vs. global), ultimately they both rely on using geochemical data that are preserved as a primary signal.

### 2.1. Geochemical redox proxies used to study the Ordovician – I/Ca, Mo and U concentrations and isotopes

#### 2.1.1. I/Ca ratios

Iodine is thermodynamically stable in two forms in most marine conditions either as iodide ($I^-$) under anoxic conditions, or iodate ($IO_3^-$) under oxic conditions (Lu et al., 2010). Iodide is incompatible in the carbonate crystal lattice, but iodate can substitute for the carbonate ion in carbonate minerals in trace amounts (Lu et al., 2010). Thus, relatively low I/Ca values can be used as evidence for periods of anoxia, which is supported if measured in parallel with other proxy data for anoxia, such as positive excursions in $\delta^{13}C$ and $\delta^{34}S$ (Lu et al., 2010; Zhou et al., 2015; Owens et al., 2017; Edwards et al., 2018). The I/Ca proxy is by nature a local redox proxy as iodine concentrations are measured from carbonate rocks (e.g., micrite), which likely precipitate directly from seawater, and thus capture a water column signal above the site of deposition. A recent study by Edwards et al. (2018) used the I/Ca proxy to show that both global and local evidence for anoxia occurs at approximately the same interval as a local extinction in Tremadocian carbonates in the Great Basin region, USA (Fig. 3). Presently this is the only study that has applied the I/Ca proxy to study anoxia in Ordovician carbonates and shows promise to be useful in other Paleozoic successions. Long-term trends in I/Ca from Precambrian rocks to the recent have also been interpreted to reflect the progressive oxygenation of the global ocean based on the relative

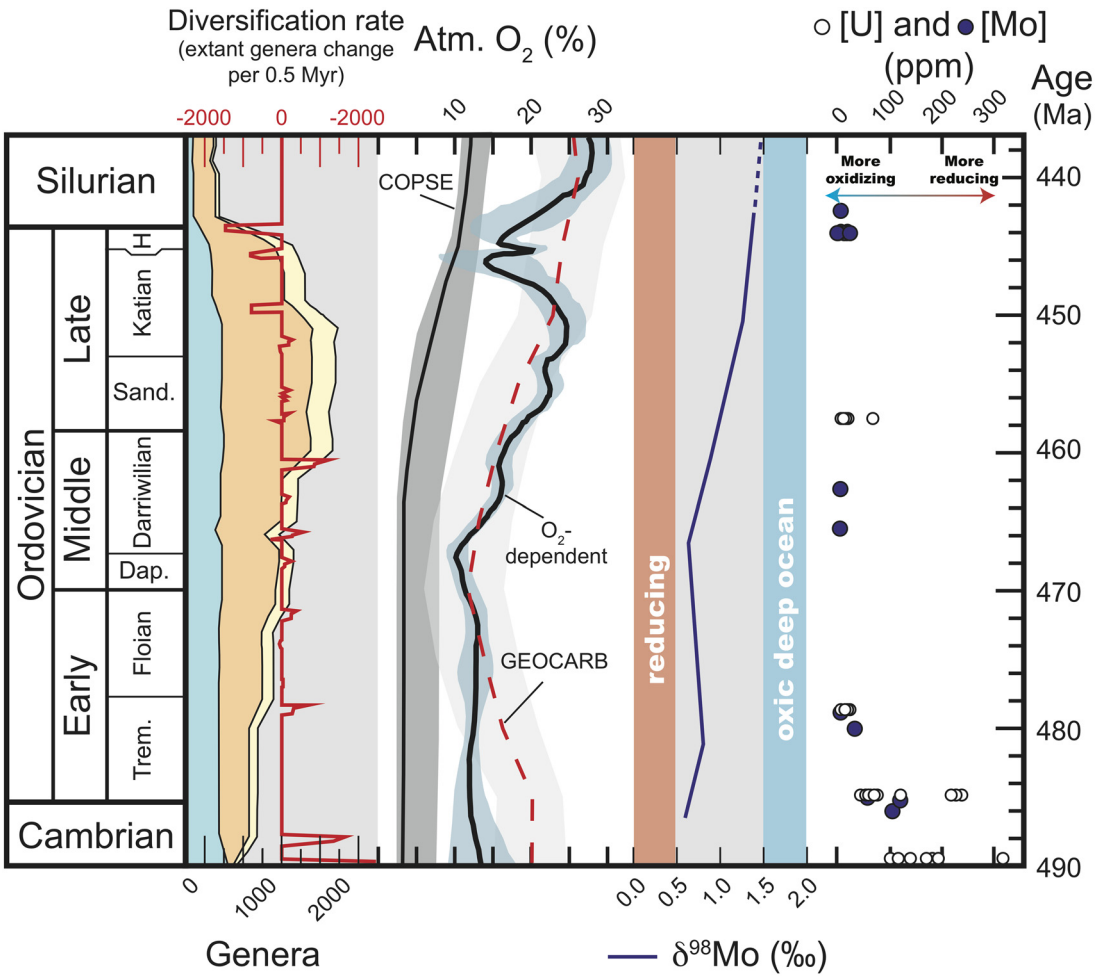


Fig. 2. Compilation of biodiversity trends and diversification rates, atmospheric $O_2$ model estimates (with respective error envelopes), and published redox-sensitive trace metal data. Biodiversity trends show total genera for the Cambrian evolutionary fauna (blue), Paleozoic evolutionary fauna (orange), and Modern evolutionary fauna (yellow) plotted with the diversification rate of all extant taxa (change in taxa per 0.5 Myr intervals). Periods of net diversification have positive diversification rates, which characterize the Early–Middle Ordovician, and periods of net extinction have negative diversification rates (latest Late Ordovician). Atmospheric $O_2$ estimates from three models (COPSE, GEOCARB, and $O_2$-dependent) all show oxygenation occurred during the Middle–Late Ordovician. Under oxic conditions, seawater $\delta^{98}$Mo values are more positive (~+2‰) and coincident with lower Mo and U concentrations (see Section 2.1.2. in the main text for further description). Biodiversity data, and oxygen modeling results ($O_2$-dependent and GEOCARB) are from Edwards et al. (2017), COPSE model results from Lenton et al. (2018), Mo isotope and concentration data from Dahl et al. (2010), and U concentration data from Hennessy and Mossman (1996), Schovsbo (2002), and Abanda and Hannigan (2006). H = Hirnantian, Sand. = Sandbian, Dap. = Dapingian, Trem. = Tremadocian, Atm. = Atmospheric. (For interpretation of the references to color in this figure legend, the reader is referred to the web version of this article.)

amount of iodine preserved in carbonate rocks, where I/Ca values are low in Archean and Proterozoic strata, increase slightly in Paleozoic strata, and finally contain near-modern values by the Mesozoic until the recent (Lu et al., 2018).

### 2.1.2. *Mo and U concentrations and isotopic ratios*

Concentrations of trace metals such as Mo and U, as well as their isotopic values, are also used to estimate periods of oxic or anoxic water column conditions. Mo and U are redox-sensitive trace metals because these metals are stable in an aqueous phase under oxic conditions (as $MoO_4^{2-}$ and $UO_2^{2-}$, respectively), but under reducing conditions these metals will adsorb or complex with dissolved sulfide or organic matter in their reduced species and deposit as sediment (Algeo, 2004; Algeo and Lyons, 2006; Weyer et al., 2008; Tissot and Dauphas, 2015; Dickson, 2017). Thus, elevated Mo and U concentrations in sedimentary successions, typically measured from fine-grained clastics like black shale facies, are interpreted to record local periods of anoxia/euxinia. However, as globally reducing conditions expand, Mo and U reservoirs are drawn down and can mute the enrichments observed for each location even under persistent euxinic conditions (Gill et al., 2011; Reinhard et al., 2013; Owens et al., 2016; Sahoo et al., 2016). Though these proxies can be useful in determining first-order changes in redox conditions in deep time (Dickson, 2017), they are highly complex where local basin effects can affect trace metal concentrations in the sediment. For example, under euxinic conditions in the restricted modern Black Sea, aqueous Mo drawdown occurs due to the formation of Mo-sulfide precipitates, but Mo concentrations in the sediment are relatively low due to restricted exchange and replenishment from the global Mo reservoir (Dickson, 2017). However, in euxinic basins with more frequent exchange and

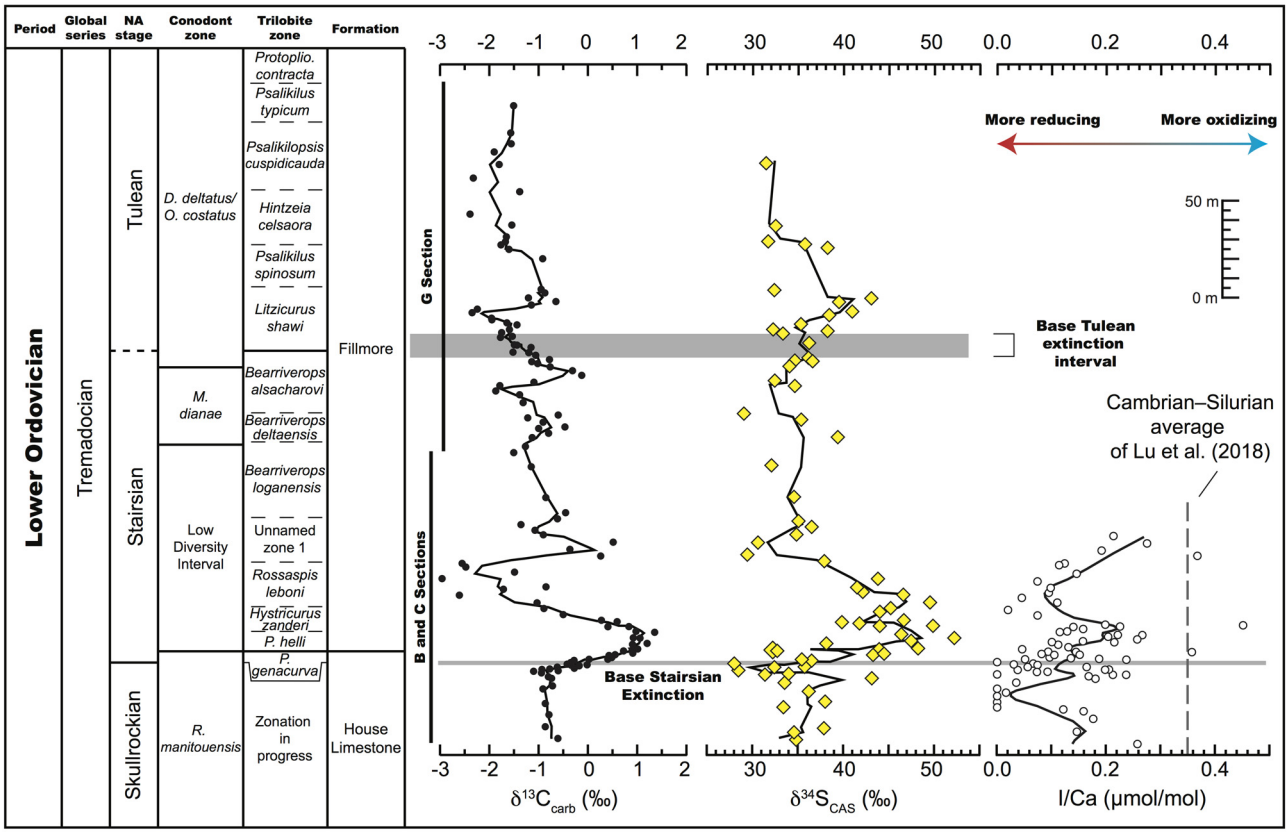


Fig. 3. New and published $\delta^{13}C$, $\delta^{34}S$, and I/Ca data from the Ibex area with most recent trilobite zonation (see Table 1 for new isotope data). The base-Stairsian trilobite extinction occurs just above the increase in $\delta^{13}C$ and $\delta^{34}S$, interpreted to record a period of global anoxia/euxinia in shallow nearshore settings (Edwards et al., 2018). The base-Tulean extinction interval can only be constrained to 12.9 m of section, which precedes a positive $\delta^{34}S$ excursion (but not $\delta^{13}C$). New $\delta^{13}C$ and $\delta^{34}S$ data are from the G-section of Hintze (1973). Published isotope and I/Ca data from the B- and C-sections (see Hintze, 1973) from Edwards et al. (2018) with the average Cambrian–Silurian I/Ca value of 0.35 μmol/mol for reference (Lu et al., 2018), trilobite zonation from Adrain et al. (2009, 2014), and conodont zonation from Ethington and Clark (1981). NA = North American.

Mo replenishment (e.g., the more open ocean Cariaco Basin), Mo concentrations in the sediment are relatively high (Lyons et al., 2009). Thus, the use of Mo and U enrichments for Ordovician black shale successions must be used with other indicators for local redox conditions (i.e., iron speciation analysis, but the isotopic composition of Mo or U, total organic carbon (TOC) concentrations, or other trace metals concentrations may also be useful) to confirm whether trace metal enrichments were due to local or global anoxic conditions and not unique to individual basin dynamics by evaluating multiple sections.

Isotopic ratios of Mo ($\delta^{97}Mo$ and $\delta^{98}Mo$) and U ($\delta^{238}U$) are used in addition to elemental concentrations to infer periods of reducing conditions. Fractionation processes are highly complex and can be imparted by both physical and biological processes, but a brief overview will be provided here (see Tissot and Dauphas (2015), Dickson (2017), and Kendall et al. (2017) for more detailed reviews). With respect to the Mo isotope system, under oxic conditions seawater is enriched in $^{98}Mo$ due to the fractionation associated with the adsorption of $^{95}Mo$ to Mn- and Fe-(oxyhydr)oxides and removal from the seawater reservoir as sediment (Arnold et al., 2004). Under highly reducing conditions (e.g., euxinia), aqueous Mo is scavenged by sulfide and organic matter, thus causing the $\delta^{98}Mo$ value of the sediment to be lower than seawater. If a basin is restricted without replenishment, such as in the modern day Black Sea, or Mo export to the sediment is highly efficient, then the $\delta^{98}Mo$ of sediment can be approximately the same as seawater (known as quantitative removal; Dickson, 2017), thus not providing strong evidence for global euxinia without other redox indicators. Non-quantitative removal of Mo will generally yield a sedimentary signature with $\delta^{98}Mo$ values less than seawater $\delta^{98}Mo$, which can occur under extremely high or low water column $H_2S$ concentrations, high pH, or open exchange with the global ocean (Dickson, 2017). Because several factors can affect $\delta^{98}Mo$, Mo isotopes are typically used in concert with other proxies to identify oxidizing and reducing conditions (e.g., Mo concentrations and TOC; Algeo and Lyons, 2006; Dickson et al., 2017). Presently the application of Mo isotopes and concentrations on Ordovician strata has yet to be as intensively studied as some Precambrian successions and Mesozoic ocean anoxic events (OAEs), but currently available data broadly and most parsimoniously indicate that Ordovician oceans became more oxygenated based on a decrease of Mo enrichment in sediment and increase of $\delta^{98}Mo$ values in deep-water shale successions (Fig. 2; Dahl et al. (2010)).

The U isotope system behaves similarly to the Mo system where $\delta^{238}U$ values of U adsorbed to Mn- and Fe-(oxyhydr)oxides are lower than oxic seawater, but several other processes can affect the fractionation of U isotopes, including

microbial activity, biogenic carbonate formation, retention in coastal margin salt marshes, and hydrothermal interaction with oceanic crust (see Weyer et al. (2008), Tissot and Dauphas (2015), and references therein). Uranium concentrations and isotopes can be measured from both fine-grained clastics, in the form of either oxides or clay minerals, and carbonate facies where U can substitute in carbonate crystal lattices. Most Ordovician studies that have measured U concentrations (but not isotopic values) have targeted black shale facies where long-term trends show that U concentrations in these shale facies decrease throughout the Ordovician (Fig. 2), which are somewhat biased in that these data are not representative of background conditions. This trend is similar to Mo enrichments and could represent local redox conditions of progressive oxygenation (or a diminishing degree of euxinic conditions), increased sedimentation rates (though highly unlikely for the duration of the Ordovician), or smaller Mo and U global inventories. A shrinking global Mo inventory, however, conflicts with long-term geochemical trends of greater sedimentary Mo concentrations with an expanding reservoir size since the Proterozoic (punctuated by short-term Mo drawdowns and euxinic events like the Steptoean positive carbon isotope excursion (SPICE) event or Mesozoic OAEs), which is thought to represent a more oxygenated global ocean (Reinhard et al., 2013). Therefore, decreasing sedimentary Mo and U concentrations throughout the Ordovician likely reflects more oxygenated oceans as persistent reducing conditions decreased. The application of U isotopes to carbonates is relatively new for Ordovician successions, but a recent investigation has applied this proxy in combination with other proxies to better understand the U isotope systematics and its application as an additional proxy for anoxic conditions during the Hirnantian Stage (Bartlett et al., 2018).

### 2.2. *Atmospheric $O_2$ modeling*

Much of the foundational work on modeling atmospheric $CO_2$ levels using $\delta^{13}C$ trends in deep time was pioneered by Robert Berner with his original GEOCARB model (Berner, 1991) and subsequent versions (Berner, 1994; Berner and Kothavala, 2001). These later versions made improvements to estimates on silicate weathering rates and volcanism as controls on $CO_2$ levels, and later $\delta^{34}S$ trends were included to estimate atmospheric $O_2$ levels (now called GEOCARBSULFvolc; Berner, 2006a, 2006b; Royer et al., 2014). In a general sense this model estimates changes in atmospheric $CO_2$ and $O_2$ using variations in long-term $\delta^{13}C$ and $\delta^{34}S$ records as proxies for organic carbon and pyrite burial rates, respectively, which are thought to be important in regulating atmospheric $CO_2$ and $O_2$ levels in their respective long-term cycles. This style of modeling has since been refined to incorporate nutrient cycling (nitrate and phosphate), known as the COPSE model (Bergman et al., 2004), and has been updated with respect to forcing factors such as rock exposure area, paleogeography, and other weathering factors (Lenton et al., 2012, 2016, 2018). An important difference between these two models is that the COPSE model includes a biological feedback system to predict organic carbon and pyrite burial rates (and thus $CO_2$ and $O_2$ levels), but the GEOCARBSULFvolc model infers these burial rates of organic carbon and pyrite based on isotope mass balance of long-term $\delta^{13}C$ and $\delta^{34}S$ trends (Lenton et al., 2018). Both models produce similar atmospheric $O_2$ trends during some portions of the Phanerozoic, namely the rise in $O_2$ levels during the Devonian followed by a Carboniferous $O_2$ high. However, some discrepancies between the models exist, namely during the early Paleozoic and Early Ordovician (Fig. 2), as well as the mid-Mesozoic (Lenton et al., 2018). Both models predict that $O_2$ levels drastically increased during the Ordovician, but the timing of this increase differs by several million years.

Another modeling approach that is independent to the GEOCARB and COPSE models uses the fractionation effect of $O_2$ on the RuBisCO enzyme during photosynthesis (referred to herein as the $O_2$-dependent model; Berner et al., 2000; Beerling et al., 2002). This modeling approach estimates changes in $O_2$ levels based on variations between primary biomass (approximated by the $\delta^{13}C$ value of bulk organic matter: $\delta^{13}C_{org}$) and the reservoir ($\delta^{13}C$ of seawater: $\delta^{13}C_{carb}$), where greater isotopic differences between the two (represented as $\delta^{13}C$, where $\delta^{13}C = \delta^{13}C_{carb} - \delta^{13}C_{org}$) represent higher $O_2$ levels, if temperature and $CO_2$ levels are considered (Berner et al., 2000; Saltzman et al., 2011; Edwards et al., 2017). This approach also includes several assumptions, namely about the composition and preservation of primary biomass, but a broadly similar trend with the GEOCARB model in the Cambrian (Saltzman et al., 2011) and Ordovician (Edwards et al., 2017) suggests that these model predictions may track a similar signal. These models use global proxies to estimate a long-term increase in $O_2$ levels, which, if true, should also be recorded in local settings, both in the form of geochemical trends and paleontological data.

## 3. Diminishing isotope excursions and marine anoxia: a case study from the ibex area, Utah, USA

The Ibex area of west-central Utah, USA has been the focus of several paleontological studies documenting the presence of late Cambrian to Middle Ordovician faunas (Hintze, 1951, 1952; Jensen, 1967; Terrell, 1973; Ethington and Clark, 1981; Holmer et al., 2005; Adrain et al., 2009, 2014), but more recently for its geochemical context to help constrain the local paleoenvironmental conditions and the stratigraphic relationship to the known faunal turnover and diversification (Marenco et al., 2013, 2016; Edwards and Saltzman, 2014, 2016; Saltzman et al., 2015; Edwards et al., 2018). A globally correlative positive $\delta^{13}C$ excursion and trilobite extinction occurs in the House Limestone and Fillmore Formation (late Tremadocian; Saltzman et al., 2015), but this excursion is significantly less pronounced in magnitude and duration compared to older excursions (Fig. 1). Edwards et al. (2018) explore this early Tremadocian $\delta^{13}C$ excursion and trilobite extinction interval further by combining I/Ca and $\delta^{34}S$ trends (measured from carbonate-associated sulfate (CAS): $\delta^{34}S_{CAS}$) from two additional sections in the Great Basin region. These authors show that this geochemical event is regionally correlative and records evidence of anoxia (possibly euxinia based on the magnitude of the $\delta^{34}S$ excursion) on both a global and local scale. Positive $\delta^{13}C$ excursions appear to end by the latest

Tremadocian (Fig. 1), but until now no high-resolution $\delta^{34}S_{CAS}$ records have been reported to document whether positive $\delta^{34}S$ excursions also end.

Previously collected carbonate rock samples were selected for geochemical analysis from the Ibex area to test whether marine anoxia, in the form of parallel positive $\delta^{13}C$ and $\delta^{34}S_{CAS}$ excursions, continues into the late Tremadocian and is present across the last major trilobite extinction event (basal Tulean Stage (Adrain et al., 2009, 2014)). Following the methods of Edwards et al. (2018), lime mudstone, wackestone, and flat pebble conglomerate lithologies were collected throughout the middle Fillmore Formation (G-section (Hintze, 1951, 1973)) at sub meter-scale resolution and processed for $\delta^{13}C$ and $\delta^{34}S_{CAS}$ (Table 1; Fig. 3). The effects of alteration to primary geochemical trends on these rocks is thought to be minimal based on isotope cross plots of $\delta^{13}C$ and $\delta^{18}O$ values, as well as from microscopic analysis using cathodoluminescence of representative facies (Edwards and Saltzman, 2014; Edwards et al., 2018). Across or just above the base Tulean trilobite extinction interval, which is poorly constrained to a shale-dominated 12.9-m-thick interval (Jonathan Adrain, pers. comm.), there is no prominent positive $\delta^{13}C$ excursion similar to the older base-Stairsian extinction. A negative $\delta^{13}C$ trend is recorded in the rocks immediately above this extinction interval, decreasing upsection from baseline values of ~-1.5‰ to −2.36‰, followed by a rapid increase to −0.66‰ (Fig. 3), which may record a small positive excursion but it is well above the extinction interval. Above and below this extinction interval, however, $\delta^{13}C$ values reach relative maxima of −0.13‰ and −0.66‰, respectively, uncharacteristic for the older excursion/extinction events where $\delta^{13}C$ increased during or immediately after the extinction event (Fig. 1).

Though $\delta^{13}C$ values do not record a positive excursion immediately following the extinction interval across the Stairsian-Tulean interval as they do at the base of the Stairsian (Fig. 3), new $\delta^{34}S_{CAS}$ data preserve a similar trend. The occurrence of a positive $\delta^{34}S_{CAS}$ excursion is similar to that of the older Stairsian excursion where the onset of the base-Tulean $\delta^{34}S_{CAS}$ excursion follows the extinction interval. Because both $\delta^{13}C_{carb}$ and $\delta^{34}S_{CAS}$ data were measured from the same section (G-section of Hintze, 1973), incorrect correlation cannot explain the decoupling of isotope trends. Above the extinction interval $\delta^{34}S_{CAS}$ values record a positive 7.7‰ excursion, about half the magnitude as the base-Stairsian $\delta^{34}S_{CAS}$ excursion. $\delta^{34}S_{CAS}$ values return to a baseline value of ~ + 30‰ until the end of the sampled section. Above this Tulean extinction, positive $\delta^{34}S_{CAS}$ excursions appear to end where $\delta^{34}S_{CAS}$ values vary around +30‰ in the Middle Ordovician Juab Formation, decreasing slightly to +20‰ in the overlying Kanosh Shale, a possibly restricted and anoxic lagoon environment, and back to ~ + 30‰ in the upper Kanosh (Marenco et al., 2013). Regional correlations are not yet possible using paired $\delta^{13}C_{carb}$–$\delta^{34}S_{CAS}$ datasets to confirm whether this base Tulean decoupling phenomenon exists elsewhere because other published data are too coarsely resolved to make meaningful correlations (e.g., Edwards et al., 2017). I/Ca ratios have not yet been measured throughout this

Table 1
Carbon and sulfur isotopic data from the Ibex area, Utah, USA.

| Sample ID | Height (m) | $\delta^{13}C_{carb}$ (‰ – VPDB) | $\delta^{34}S_{CAS}$ (‰ – VCDT) |
|---|---|---|---|
| LDN7365 | 111.28 | −0.60 | 34.77 |
| LDN7367 | 114.33 | | 34.60 |
| LDN7369 | 117.38 | −0.85 | 37.77 |
| LDN7373 | 123.47 | −0.80 | |
| LDN7376 | 128.05 | | 33.55 |
| LDN7377 | 129.57 | −0.85 | 38.11 |
| LDN7381 | 135.67 | −0.88 | 36.49 |
| LDN7382 | 137.19 | −0.90 | |
| LDN7383 | 138.72 | −0.71 | 33.61 |
| LDN7385 | 141.77 | −0.72 | 42.95 |
| LDN7385.1 | 141.77 | | 43.15 |
| LDN7386 | 143.29 | −0.80 | |
| LDN7387 | 144.82 | −0.94 | 34.15 |
| B-TOP7396 | 145.26 | −0.78 | 31.52 |
| B-TOP7397 | 146.01 | −1.10 | 28.51 |
| LDN7388 | 146.34 | −0.59 | |
| B-TOP7398 | 146.76 | −0.93 | |
| B-TOP7399 | 147.51 | −0.77 | |
| LDN7389 | 147.86 | −0.27 | |
| B-TOP7400 | 148.26 | −0.63 | 32.45 |
| B-TOP7401 | 149.01 | −0.17 | 28.20 |
| LDN7390 | 149.39 | −0.34 | |
| C65-7541 | 149.41 | −0.03 | |
| B-TOP7402 | 149.76 | −0.27 | 35.95 |
| B-TOP7403 | 150.51 | −0.42 | |
| LDN7391 | 150.91 | 0.02 | 36.72 |
| B-TOP7391.1 | 150.91 | | 35.80 |
| B-TOP7404 | 151.26 | −0.33 | |
| B-TOP7405 | 152.01 | −0.27 | |
| C65-7543 | 152.46 | 0.42 | |
| B-TOP7406 | 152.76 | 0.02 | |
| B-TOP7407 | 153.51 | 0.51 | |
| LDN7393 | 153.96 | 0.55 | |
| B-TOP7408 | 154.26 | 0.43 | |
| B-TOP7409 | 155.01 | | 43.28 |
| C65-7545 | 155.51 | 0.94 | |
| B-TOP7410 | 155.76 | 0.91 | 44.50 |
| B-TOP7411 | 156.51 | 0.77 | |
| LDN7395 | 157.01 | 1.03 | 32.39 |
| LDN7395.1 | 157.00 | | 32.65 |
| C65-7530 | 157.01 | 0.72 | |
| B-TOP7412 | 157.26 | 0.92 | |
| B-TOP7413 | 158.01 | | 44.09 |
| B-TOP7414 | 158.76 | | 48.29 |
| B-TOP7415 | 159.51 | | 38.28 |
| C65-7533 | 160.06 | 0.91 | 47.62 |
| B-TOP7416 | 160.26 | 1.23 | |
| C65-7534 | 163.11 | 0.94 | |
| B-TOP7420 | 163.26 | 1.06 | 52.15 |
| C65-7536 | 166.16 | 1.00 | |
| B-TOP7424 | 166.26 | 1.36 | 46.36 |
| C65-7538 | 169.21 | 0.85 | |
| B-TOP7427 | 168.51 | | 43.96 |
| B-TOP7428 | 169.26 | 0.40 | 49.92 |
| B-TOP7430 | 170.76 | | 46.86 |
| B-TOP7431 | 171.51 | 0.60 | 39.99 |
| B-TOP7431.1 | 171.51 | | 41.81 |
| C65-7540 | 172.26 | 0.28 | |
| C65-5253 | 175.30 | −0.50 | 43.95 |
| C65-5254 | 178.35 | −0.88 | 45.28 |
| C65-5255 | 181.71 | −1.05 | 49.56 |
| C65-5256 | 185.06 | −2.60 | 46.54 |

Table 1 (*Continued*)

| Sample ID | Height (m) | $\delta^{13}C_{carb}$ (‰ – VPDB) | $\delta^{34}S_{CAS}$ (‰ – VCDT) |
|---|---|---|---|
| C65-5257 | 187.50 | −1.72 | 42.17 |
| C65-5258 | 189.94 | −0.86 | 41.61 |
| C65-5259 | 193.60 | −2.97 | 43.83 |
| C65-5260 | 196.95 | −1.49 | |
| C65-5261 | 201.22 | −2.47 | |
| C65-5262 | 202.74 | −2.54 | 37.98 |
| C65-5263 | 205.79 | 0.25 | 29.51 |
| C65-5264 | 208.84 | −0.35 | |
| C65-5265 | 212.50 | 0.51 | 30.64 |
| C65-5266 | 215.85 | −0.92 | |
| C65-5267 | 217.99 | −1.04 | 34.82 |
| C65-5268 | 221.04 | −1.36 | 36.50 |
| C65-5269 | 224.09 | −0.61 | 35.06 |
| C65-5270 | 227.13 | −0.43 | |
| C65-5273 | 236.28 | −0.86 | 34.65 |
| C65-5278 | 252.13 | −1.16 | 32.11 |
| C65-5281 | 260.67 | −1.50 | |
| C65-5282 | 263.72 | −1.25 | |
| C65-5283 | 266.77 | −1.14 | 39.41 |
| C65-5284 | 269.82 | −0.79 | |
| G-7432 | 271.60 | −1.01 | |
| C65-5285 | 272.87 | −0.47 | |
| C65-5286 | 275.91 | −0.86 | |
| G-7436 | 277.60 | −1.23 | 35.34 |
| C65-5287 | 278.96 | −0.61 | 28.93 |
| G-7441 | 285.10 | −1.33 | |
| G-7444 | 289.60 | −1.40 | |
| G-7445 | 291.10 | −1.86 | |
| G-7446 | 292.60 | −1.76 | |
| G-7447 | 294.10 | −1.77 | 34.68 |
| G-7448 | 295.60 | −1.11 | 32.46 |
| G-7450 | 298.60 | −0.13 | |
| G-7452 | 301.60 | −0.33 | |
| G-7453 | 303.10 | −0.76 | |
| G-7454 | 304.60 | −1.01 | 34.23 |
| G-7455 | 306.10 | −1.12 | 34.70 |
| G-7456 | 307.60 | −0.79 | 36.59 |
| G-7457 | 309.10 | −1.06 | 36.23 |
| G-7458 | 310.60 | −1.22 | |
| G-7459 | 312.10 | −1.50 | |
| G-7460 | 313.60 | −1.18 | |
| G-7461 | 315.10 | −1.43 | 36.03 |
| G-7462 | 316.60 | −1.51 | |
| G-7463 | 318.10 | −1.76 | |
| G-7464 | 319.60 | −1.55 | |
| G-7465 | 321.10 | −1.74 | 33.35 |
| G-7466 | 322.60 | | 38.34 |
| G-7467 | 324.10 | −1.57 | 32.37 |
| G-7468 | 325.60 | −1.46 | 35.49 |
| G-7469 | 327.10 | −1.66 | |
| G-7470 | 328.60 | −1.93 | |
| G-7471 | 330.10 | −1.96 | 38.48 |
| G-7472 | 331.60 | −2.36 | 40.90 |
| G-7473 | 333.10 | −2.23 | |
| G-7474 | 334.60 | −1.13 | |
| G-7475 | 336.10 | −1.13 | |
| G-7476 | 337.60 | −0.66 | 39.60 |
| G-7477 | 339.10 | −1.22 | 43.14 |
| G-7479 | 342.10 | −0.89 | |
| G-7480 | 343.60 | −0.95 | 32.49 |
| G-7480.1 | 359.35 | −0.93 | |
| G-7480.2 | 363.10 | −1.56 | |
| G-7480.3 | 364.60 | −1.61 | |
| G-7480.4 | 365.60 | −1.76 | 38.32 |

Table 1 (*Continued*)

| Sample ID | Height (m) | $\delta^{13}C_{carb}$ (‰ – VPDB) | $\delta^{34}S_{CAS}$ (‰ – VCDT) |
|---|---|---|---|
| G-7480.5 | 367.60 | −1.68 | 35.77 |
| G-7480.6 | 369.10 | −1.58 | 31.59 |
| G-7480.7 | 370.60 | −1.67 | |
| G-5288 | 376.60 | −1.57 | 32.54 |
| G-5289 | 382.60 | −2.40 | |
| G-5291 | 394.60 | −1.38 | |
| G-5292 | 400.60 | −2.32 | |
| G-5293 | 408.60 | −1.81 | 31.67 |

base Tulean interval, which could confirm whether the local water column was anoxic at Ibex.

## 4. Discussion

### *4.1. Oxygenation of the Paleozoic ocean*

The strongly coupled nature between the SPICE and base-Stairsian positive $\delta^{13}C$ and $\delta^{34}S_{CAS}$ excursions appears to end by the end of the Tremadocian during the Tulean Stage. Major positive $\delta^{13}C$ excursions also appear to end after these Tremadocian excursions until the Late Ordovician (Bergström et al., 2010; Young et al., 2010). Long-term $\delta^{13}C$ stability following the late Cambrian SPICE event and throughout the Ordovician has been interpreted to represent a period of nitrogen limitation and diminished productivity globally that ended major increases in organic carbon burial (Saltzman, 2005). This model presumes that the decrease in frequency and magnitude of $\delta^{13}C$ excursions is caused by ocean stagnation under a warm greenhouse climate that limited upwelling of nutrients and promoted marine anoxia in the deep ocean. With decreased primary production under anoxic conditions globally, burial rates of organic carbon (and pyrite) would be more muted, thus not producing major positive $\delta^{13}C$ (and $\delta^{34}S$) excursions.

Sulfur isotopic trends of CAS measured from Lower–Middle Ordovician carbonates also support the notion that a stratified ocean with reducing (anoxic to euxinic) deep waters was dynamically maintained and decoupled from the surface ocean during the Ordovician (Kah et al., 2016). Kah et al. (2016) use a two-reservoir box model to explore how a stratified ocean with regional euxinic conditions was maintained to produce observed $\delta^{34}S_{CAS}$ trends in their study. Quantitative estimates for atmospheric $O_2$ levels in the ocean-atmosphere system, however, suggest that the Early Ordovician had atmospheric $O_2$ levels about 13% of the atmospheric composition (or 60% of the modern), but near-modern $O_2$ levels were achieved by the Middle–Late Ordovician (~25%; Fig. 2). These estimates utilize a modified version of the GEOCARBSULFvolc base model (Royer et al., 2014) that uses isotope mass balance of $\delta^{13}C$ and $\delta^{34}S$ trends to estimate $O_2$ levels, as well as an $O_2$-dependence approach (Berner et al., 2000) that estimates atmospheric $O_2$ using differences in the fractionation between seawater dissolved inorganic carbon (DIC) and primary biomass (phytoplankton) when corrected for temperature, $CO_2$ levels, and secondary effects to organic matter. The COPSE model,

a model that estimates $O_2$ and $CO_2$ levels based on assumed weathering rates and phosphate delivery to the ocean to fuel primary productivity in phosphate-limited oceans (among several other factors), also predicts that atmospheric $O_2$ levels were low during the Early Ordovician (3–5%) but later increased to ~13% by the end of the Ordovician (Lenton et al., 2018).

These three atmospheric $O_2$ modeling studies are seemingly in some conflict with each other as they predict a different rate and degree of oxygenation of the early Paleozoic ocean-atmosphere system. These models are either based on geochemical data that are assumed to represent an averaged global value (the GEOCARB and $O_2$-dependent models) or globally averaged weathering/burial rates (COPSE model). If an oxycline was maintained in the global ocean due to sluggish circulation that created water masses in disequilibrium with each other, then these models may be tracking signals that do not represent the true global average. As the global ocean became progressively oxygenated under this scenario, this would have depressed the oxycline deeper within the water column and ultimately prevented oxygen minimum zones (OMZs) from expanding into shallow shelf settings during relative sea-level rises to cause extinctions of benthic fauna (Fig. 4). Reducing conditions in some isolated basins analogous to the modern day Cariaco Basin likely persisted throughout the Silurian and into the Devonian as evidenced by positive $\delta^{13}C$ and $\delta^{34}S$ excursions thought to record intermittent periods of increased rates of organic and pyrite burial in Silurian strata (Kleinberg et al., 2016; Bowman et al., 2017).

Sluggish ocean circulation likely continued throughout the early Paleozoic (with the possible exception of the Hirnantian glaciation), due to a diminished equator-to-pole thermal gradient under greenhouse conditions (Saltzman, 2005) that could sustain an oxycline within the water column without vigorous circulation and deep water formation. The oceans appear to have ultimately been ventilated by the Devonian (Dahl et al., 2010; Lenton et al., 2018), perhaps due to the proliferation of land plants that elevated atmospheric $O_2$ levels, as the oxycline was finally depressed into the sediment profile in the deep ocean. Global cooling may have also contributed to ventilating the oceans as land plants removed $CO_2$ from the atmosphere to weaken the greenhouse effect, which may have invigorated global circulation from a stronger equator-to-pole thermal gradient such that deep-water formation at the surface further oxygenated the deep ocean.

### 4.2. Oxygenation and Ordovician biodiversification

Several biologic and environmental events throughout the Ordovician are thought to be causes of the biodiversification that represents the GOBE (see Harper et al., 2015 for an in-depth review). Based on an increase in the amount of skeletal material that comprises Cambro-Ordovician carbonates, Pruss et al. (2010) speculate that energetic costs associated with biomineralization of carbonate were lowered during the Ordovician due to a stronger carbonate saturation gradient. A stronger gradient could form in more oxygenated surface waters as primary production invigorated the biologic pump and removed more $CO_2$ (a weak acid) from surface waters. This notion is supported by models that indicate that $O_2$ levels approximately doubled by the end Ordovician (Lenton et al., 2016, 2018; Edwards et al., 2017). A rapid $O_2$ increase coincides with a major increase in global biodiversity (Fig. 2), which Edwards et al. (2017) interpret as an important driver of the GOBE. The highest biodiversity levels coincide with the highest $O_2$ levels during the mid Late Ordovician, both of which decrease prior to the Hirnantian and may reflect a previously unrecognized driver of the Hirnantian mass extinction.

New geochemical analyses and modeling studies continue to provide evidence supporting the link between $O_2$ levels and biodiversity. The late Cambrian represents a time when the persistent incursion of anoxic-euxinic waters into shallow shelf settings caused the extinction of trilobites (e.g., Gill et al., 2011), likely in addition to other taxa like conodonts (e.g., Ethington and Clark, 1981), and hindered global biodiversification. As the Cambrian–Ordovician ocean-atmosphere system became progressively oxygenated, the area along the shelf experiencing anoxic conditions decreased (Fig. 4). Following these extinctions and isotope excursions, biodiversity levels begin to gradually increase throughout the Floian Stage (Fig. 2). By the Middle Ordovician, biodiversity levels increased at higher rates that also coincide with the first major pulse of atmospheric $O_2$. Major perturbations to the carbon cycle are not as frequent at this time, suggesting that organic burial rates were relatively constant. This could be explained by either the diminished extent of OMZs or because upwelling of nutrient-rich deep water above areas of the seafloor under an OMZ was limited under a sluggishly circulating global ocean (Saltzman, 2005). Atmospheric $O_2$ levels remained high throughout the Late Ordovician, although there is some disagreement between models across the end Ordovician mass extinction (Fig. 2). The COPSE and GEOCARB models predict that $O_2$ levels increased or remained constant across the Hirnantian extinction, but these models bin geochemical data in 5–10 Myr time steps that may smooth out rapid (<1 Myr) perturbations. The $O_2$-dependent model, however, uses a <0.1 Myr time step for estimated $O_2$ levels and predicts a major $O_2$ drop that coincides with a decline in global biodiversity levels, suggesting that an $O_2$ decrease contributed to this extinction.

## 5. Future directions

Though significant advances have been made in the past few decades to better constrain the co-evolution of early Paleozoic environmental conditions and bioevents, several uncertainties remain that should be the focus of future studies to continue efforts to better understand this critical period of Earth's history:

1. Model estimates of atmospheric $O_2$ are not in good agreement with each other throughout the Tremadocian–Floian (Early Ordovician) interval (Fig. 2). The GEOCARB model, for example, estimates that atmospheric $O_2$ levels were near modern concentrations and significantly more than the COPSE and $O_2$-dependent models. GEOCARB $O_2$ estimates are sensitive to changes in the $\delta^{34}S$ value of the global sul-

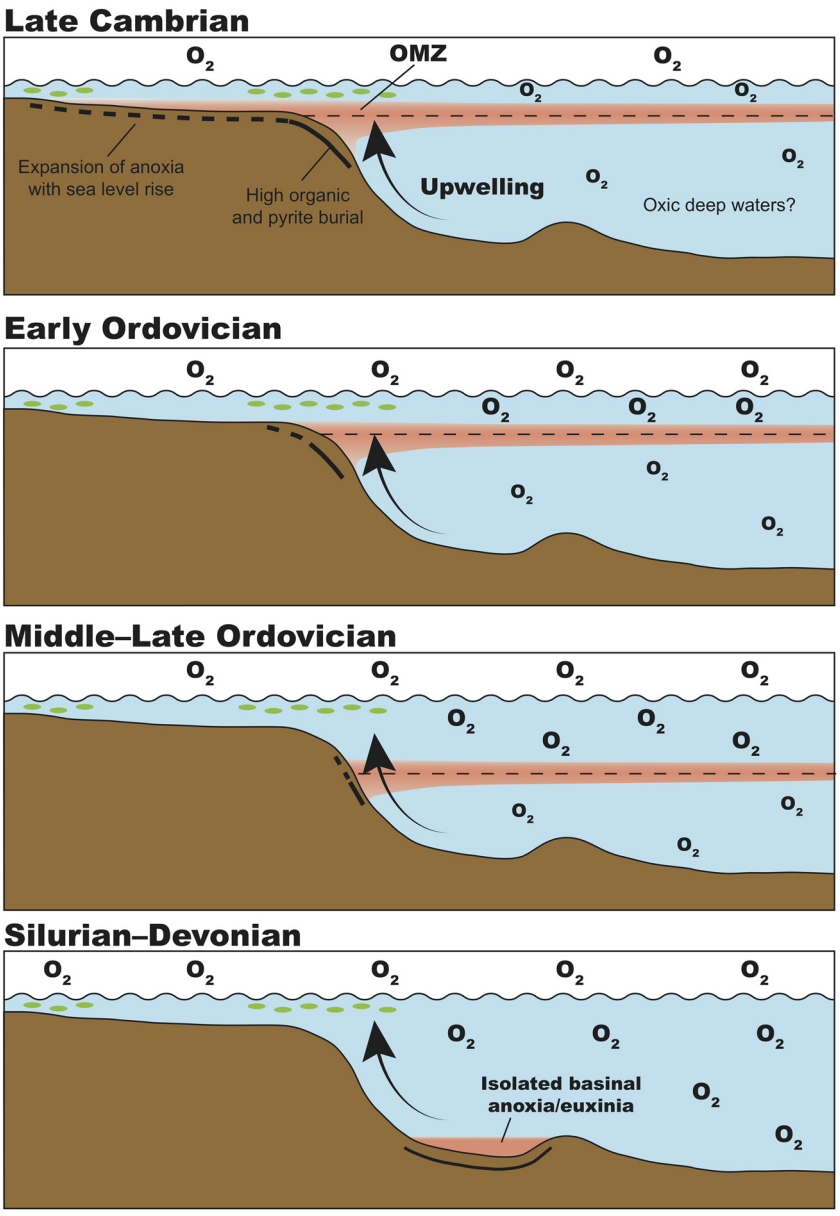


Fig. 4. Schematic progression of the oxygenation of atmosphere and surface ocean from the late Cambrian to Devonian. During the Cambrian and Early Ordovician, a subsurface oxygen minimum zone (OMZ) is thought to surround large paleocontinent landmasses (e.g., Laurentia), which expanded into shallow shelf environments during sea level rises. The incursion of OMZs into nearshore settings during a relative sea level rise would increase extinction rates of benthic faunas (i.e., trilobites) and create wider anoxic regions on the seafloor (dashed lines) that increased organic carbon and pyrite burial rates (i.e., large $\delta^{13}C$ excursions). Upwelling and nutrient delivery from rivers would promote primary productivity in shallow waters (green ovals), which would likely be buried if regions of high primary productivity rates were located over portions of the seafloor under an OMZ. As $O_2$ levels increased and reduced the anoxic fraction of the water column during the Ordovician, OMZs were driven deeper in the water column and diminished the areal seafloor extent that experienced anoxia, thus decreasing the frequency and magnitude of isotopic excursions. Periodic $\delta^{13}C$ and $\delta^{34}S$ excursions continue until the Devonian where anoxic/euxinic bottom waters in isolated basins persisted and increased organic carbon and pyrite burial with pulses of high primary productivity in the overlying surface waters. (For interpretation of the references to color in this figure legend, the reader is referred to the web version of this article.)

fate reservoir, which is poorly constrained throughout this interval. If the marine sulfate reservoir was isotopically heterogeneous (cf. Thompson and Kah, 2012), then GEOCARB $O_2$ estimates could be inaccurate if $\delta^{34}S$ values used in previous studies were not representative of the global $\delta^{34}S$ reservoir. Better constraints on the global sulfate $\delta^{34}S$ record may help to reconcile differences between model estimates.

2. The Darriwilian–Sandbian interval represents an important period with respect to both the biosphere and geochemical cycles. Brachiopod diversity, for example, experienced a major increase during the Darriwilian, and at different times on separate paleocontinents (Harper et al., 2015; Trubovitz and Stigall, 2016). Coincident with this diversification $O_2$ levels appear to sharply increase (Fig. 2), sea surface temperatures may have cooled enough to be tolerable for temperature-sensitive fauna (Trotter et al., 2008), as well as a major drop in strontium isotopes (Saltzman et al., 2014) that reflect changes in silicate weathering rates and

rock type (Young et al., 2009), which may have delivered more nutrients to shallow shelf environments. Greater focus on this interval aimed at producing more highly resolved geochemical trends and environmental conditions should help to resolve which environmental drivers, if any at all, were critical for the major pulse of biodiversity during this interval.

3. Was there an "oxygen crisis" leading up to the end Ordovician (Fig. 2), that contributed to the Late Ordovician mass extinction, or were $O_2$ levels sufficiently high and had no effect on the biodiversity decline? Oceans are generally thought to become *more* oxygenated during glacial episodes because cooler oceans can hold more dissolved $O_2$ and invigorated global circulation and deep-water formation would deliver more oxygenated surface waters to the seafloor, which ultimately upwell onto continental shelves. Though this "oxygen crisis" is in good temporal agreement with a decrease in biodiversity, these $O_2$ estimates come from geochemical data measured from carbonate successions with poorly constrained biostratigraphic age estimates. Future work aimed at acquiring temporally resolved paired $\delta^{13}C$ values from carbonate and bulk organic matter (including the $\delta^{13}C$ of individual biomarkers) from late Katian to Hirnantian strata could clarify whether this "oxygen crisis" is real or merely an artifact of using this particular approach during this interval.

## Acknowledgements

I thank Matthew Saltzman for valuable discussion on an earlier version of this manuscript, as well as Jeremy Owens and an anonymous reviewer for their constructive reviews. Jonathan Adrain and Stephen Westrop are acknowledged for their contributions in the trilobite biostratigraphy in the Ibex area. Jennifer Houghton and Stephanie Moore are thanked for providing laboratory assistance, as well as David Fike for use of his laboratory for sulfur isotopic analysis at Washington University in St. Louis. Funding was provided in part by support from the Packard Foundation to David Fike. This paper is a contribution to IGCP Project 653 "The onset of the Great Ordovician Biodiversification Event".

## References

Abanda, P.A., Hannigan, R.E., 2006. Effect of diagenesis on trace element partitioning in shales. Chemical Geology 230, 42–59.

Adrain, J.M., McAdams, N.E.B., Westrop, S.R., 2009. Trilobite biostratigraphy and revised bases of the Tulean and Blackhillsian Stages of the Ibexian Series, Lower Ordovician, western United States. Memoirs of the Association of Australasian Palaeontologists 37, 541–610.

Adrain, J.M., Westrop, S.R., Karim, T.S., Landing, E., 2014. Trilobite biostratigraphy of the Stairsian Stage (upper Tremadocian) of the Ibexian Series, Lower Ordovician, western United States. Memoirs of the Association of Australasian Palaeontologists 45, 167–214.

Algeo, T.J., 2004. Can marine anoxic events draw down the trace element inventory of seawater? Geology 32, 1057–1060.

Algeo, T.J., Lyons, T.W., 2006. Mo – total organic carbon covariation in modern anoxic marine environments: Implications for analysis of paleoredox and paleohydrographic conditions. Paleoceanography and Paleoclimatology 21 (1), http://dx.doi.org/10.1029/2004PA001112.

Anbar, A.D., Knoll, A.H., 2002. Proterozoic ocean chemistry and evolution: a bioinorganic bridge? Science 297, 1137–1142.

Arnold, G.L., Anbar, A.D., Barling, J., Lyons, T.W., 2004. Molybdenum isotope evidence for widespread anoxia in mid-Proterozoic oceans. Science 304, 87–90.

Bachan, A., Lau, K.V., Saltzman, M.R., Thomas, E., Kump, L.R., Payne, J.L., 2017. A model for the decrease in amplitude of carbon isotope excursions across the Phanerozoic. American Journal of Science 317, 641–676.

Bartlett, R., Elrick, M., Wheeley, J.R., Polyak, V., Desrochers, A., Asmerom, Y., 2018. Abrupt global-ocean anoxia during the Late Ordovician–early Silurian detected using uranium isotopes of marine carbonates. Proceedings of the National Academy of Sciences 115, 5896–5901.

Beerling, D.J., Lake, J.A., Berner, R.A., Hickey, L.J., Taylor, D.W., Royer, D.L., 2002. Carbon isotope evidence implying high $O_2/CO_2$ ratios in the Permo-Carboniferous atmosphere. Geochimica et Cosmochimica Acta 66, 3757–3767.

Bergman, N.M., Lenton, T.M., Watson, A.J., 2004. COPSE: a new model of biogeochemical cycling over Phanerozoic time. American Journal of Science 304, 397–437.

Bergström, S.M., Young, S., Schmitz, B., 2010. Katian (Upper Ordovician) $\delta^{13}C$ chemostratigraphy and sequence stratigraphy in the United States and Baltoscandia: A regional comparison. Palaeogeography, Palaeoclimatology, Palaeoecology 296, 217–234.

Berner, R.A., 1991. A model for atmospheric $CO_2$ over Phanerozoic time. American Journal of Science 291, 339–376.

Berner, R.A., 1994. GEOCARB II: a revised model of atmospheric $CO_2$ over Phanerozoic time. American Journal of Science 294, 56–91.

Berner, R.A., 2006a. GEOCARBSULF: a combined model for Phanerozoic atmospheric $O_2$ and $CO_2$. Geochimica et Cosmochimica Acta 70, 5653–5664.

Berner, R.A., 2006b. Inclusion of the weathering of volcanic rocks in the GEOCARBSULF model. American Journal of Science 306, 295–302.

Berner, R.A., Kothavala, Z., 2001. GEOCARB III: a revised model of atmospheric $CO_2$ over Phanerozoic time. American Journal of Science 301, 182–204.

Berner, R.A., Petsch, S.T., Lake, J.A., Beerling, D.J., Popp, B.N., Lane, R.S., Laws, E.A., Westley, M.B., Cassar, N., Woodward, F.I., Quick, W.P., 2000. Isotope fractionation and atmospheric oxygen: implications for Phanerozoic $O_2$ evolution. Science 287, 1630–1633.

Berner, R.A., VandenBrooks, J.M., Ward, P.D., 2007. Oxygen and evolution. Science 316, 557–558.

Bowman, C.N., Young, S.A., Owens, J.D., Kaljo, D., Hints, O., Martma, T., 2017. Oceanographic redox changes associated with the late Silurian Lau extinction event: new geochemical evidence from the Priekule-20 drill core, Latvia. Geological Society of America Abstracts with Programs 49, No. 6, https://doi.org/10.1130/abs/2017AM-303213.

Buggisch, W., Keller, M., Lehnert, O., 2003. Carbon isotope record of Late Cambrian to Early Ordovician carbonates of the Argentine Precordillera. Palaeogeography, Palaeoclimatology, Palaeoecology 195, 357–373.

Butterfield, N.J., 2011. Animals and the invention of the Phanerozoic Earth system. Trends in Ecology and Evolution 26, 81–87.

Canfield, D.E., Lyons, T.W., Raiswell, R., 1996. A model for iron deposition to euxinic black sea sediments. American Journal of Science 296, 818–834.

Chen, X., Ling, H.F., Vance, D., Shields-Zhou, G.A., Zhu, M., Poulton, S.W., Och, L.M., Jiang, S.Y., Li, D., Cremonese, L., Archer, C., 2015. Rise to modern levels of ocean oxygenation coincided with the Cambrian radiation of animals. Nature Communications 6, 1–7.

Cloud, P.E., 1968. Atmospheric and hydrospheric evolution on the primitive earth. Science 160, 729–736.

Cramer, B.D., Saltzman, M.R., 2005. Sequestration of $^{12}C$ in the deep ocean during the early Wenlock (Silurian) positive carbon isotope excursion. Palaeogeography, Palaeoclimatology, Palaeoecology 219, 333–349.

Cramer, B.D., Saltzman, M.R., 2007. Early Silurian paired $\delta^{13}C_{carb}$ and $\delta^{13}C_{org}$ analyses from the Midcontinent of North America: implications for paleoceanography and paleoclimate. Palaeogeography, Palaeoclimatology, Palaeoecology 256, 195–203.

Dahl, T.W., Hammarlund, E.U., Anbar, A.D., Bond, D.P.G., Gill, B.C., Gordon, G.W., Knoll, A.H., Nielsen, A.T., Schovsbo, N.H., Canfield, D.E., 2010.

Devonian rise in atmospheric oxygen correlated to the radiations of terrestrial plants and large predatory fish. Proceedings of the National Academy of Sciences of the United States of America 107, 17911–17915.

Dahl, T.W., Boyle, R.A., Canfield, D.E., Connelly, J.N., Gill, B.C., Lenton, T.M., Bizzarro, M., 2014. Uranium isotopes distinguish two geochemically distinct stages during the later Cambrian SPICE event. Earth and Planetaty Science Letters 401, 313–326.

Dickson, A.J., 2017. A molybdenum-isotope perspective on Phanerozoic deoxygenation events. Nature Geoscience 10, 721–726.

Dickson, A.J., Jenkyns, H.C., Porcelli, D., van den Boorn, S., Idiz, E., 2016. Basin-scale controls on the molybdenum-isotope composition of seawater during Oceanic Anoxic Event 2 (Late Cretaceous). Geochimica et Cosmochimica Acta 178, 291–306.

Dickson, A.J., Gill, B.C., Ruhl, M., Jenkyns, H.C., Porcelli, D., Idiz, E., Lyons, T.W., van den Boorn, S.H.J.M., 2017. Molybdenum-isotope chemostratigraphy and paleoceanography of the Toarcian Oceanic Anoxic Event (Early Jurassic). Paleoceanography 32, 813–829.

Edwards, C.T., Saltzman, M.R., 2014. Carbon isotope ($\delta^{13}C_{carb}$) stratigraphy of the Lower–Middle Ordovician (Tremadocian–Darriwilian) in the Great Basin, western United States: implications for global correlation. Palaeogeography, Palaeoclimatology, Palaeoecology 399, 1–20.

Edwards, C.T., Saltzman, M.R., 2016. Paired carbon isotopic analysis of Ordovician bulk carbonate ($\delta^{13}C_{carb}$) and organic matter ($\delta^{13}C_{org}$) spanning the Great Ordovician Biodiversification Event. Palaeogeography, Palaeoclimatology, Palaeoecology 458, 102–117.

Edwards, C.T., Saltzman, M.R., Royer, D.L., Fike, D.A., 2017. Oxygenation as a driver of the Great Ordovician Biodiversification Event. Nature Geoscience 10, 925–959.

Edwards, C.T., Fike, D.A., Saltzman, M.R., Lu, W., Lu, Z., 2018. Evidence for local and global redox conditions at an Early Ordovician (Tremadocian) mass extinction. Earth and Planetary Science Letters 481, 125–135.

Elrick, M., Polyak, V., Algeo, T.J., Romaniello, S., Asmerom, Y., Herrmann, A.D., Anbar, A.D., Zhao, L., Chen, Z., 2017. Global-ocean redox variation during the middle–late Permian through Early Triassic based on uranium isotope and Th/U trends of marine carbonates. Geology 45, 163–166.

Erbacher, J., Friedrich, O.A., Wilson, P.A., Birch, H., Mutterlose, J., 2005. Stable organic carbon isotope stratigraphy across Oceanic Anoxic Event 2 of Demerara Rise, western tropical Atlantic. Geochemistry, Geophysics, Geosystems 6, Q06010, https://doi.org/10.1029/2004GC000850.

Ethington, R.L., Clark, D.L., 1981. Lower and Middle Ordovician conodonts from the Ibex area western Millard County, Utah. Brigham Young University Geology Studies 28, 1–155.

Frei, R., Gaucher, C., Poulton, S.W., Canfield, D.E., 2009. Fluctuations in Precambrian atmospheric oxygenation recorded by chromium isotopes. Nature 461, 250–253.

Gill, B.C., Lyons, T.W., Saltzman, M.R., 2007. Parallel, high-resolution carbon and sulfur isotope records of the evolving Paleozoic marine sulfur reservoir. Palaeogeography, Palaeoclimatology, Palaeoecology 256, 156–173.

Gill, B.C., Lyons, T.W., Young, S.A., Kump, L.R., Knoll, A.H., Saltzman, M.R., 2011. Geochemical evidence for widespread euxinia in the later Cambrian ocean. Nature 469, 80–83.

Hammarlund, E.U., Dahl, T.W., Harper, D.A.T., Bond, D.P.G., Nielsen, A.T., Bjerrum, C.J., Schovsbo, N.H., Schönlaub, H.P., Zalasiewicz, J.A., Canfield, D.E., 2012. A sulfidic driver for the end-Ordovician mass extinction. Earth and Planetary Science Letters 331–332, 128–139.

Hardisty, D.S., Lu, Z., Bekker, A., Diamond, C.W., Gill, B.C., Jiang, G., Kah, L.C., Knoll, A.H., Loyd, S.J., Osburn, M.R., Planavsky, N.J., Wang, C., Zhou, X., Lyons, T.W., 2017. Perspectives on Proterozoic surface ocean redox from iodine contents in ancient and recent carbonate. Earth and Planetary Science Letters 463, 159–170.

Harper, D.A.T., Zhan, R.B., Jin, J., 2015. The Great Ordovician Biodiversification Event: reviewing two decades of research on diversity's big bang illustrated by mainly brachiopod data. Palaeoworld 24, 75–85.

Hennessy, J.F., Mossman, D.J., 1996. Geochemistry of Ordovician black shales at Meductic southern Miramichi Highlands, New Brunswick. Atlantic Geology 32, 233–245.

Hintze, L.F., 1951. Lower Ordovician detailed stratigraphic sections for western Utah. Utah Geological and Mineralogical Survey 39, 1–99.

Hintze, L.F., 1952. Lower Ordovician trilobites from western Utah and eastern Nevada. Utah Geological and Mineralological Survey 48, 1–249.

Hintze, L.F., 1973. Lower and Middle Ordovician stratigraphic sections in the Ibex area Millard County, Utah. Brigham Young University Geology Studies 20, 3–36.

Holmer, L.E., Popov, L.E., Streng, M., Miller, J.F., 2005. Lower Ordovician (Tremadocian) lingulate brachiopods from the House and Fillmore formations, Ibex Area, Western Utah, USA. Journal of Paleontology 79, 884–906.

Jensen, R.G., 1967. Ordovician brachiopods from the Pogonip Group of Millard County, western Utah. Brigham Young University Geology Studies 14, 67–100.

Jones, D.S., Fike, D.A., 2013. Dynamic sulfur and carbon cycling through the end-Ordovician extinction revealed by paired sulfate-pyrite $\delta^{34}S$. Earth and Planetary Science Letters 363, 144–155.

Jones, D.S., Fike, D.A., Finnegan, S., Fischer, W.W., Schrag, D.P., McCay, D., 2011. Terminal Ordovician carbon isotope stratigraphy and glacioeustatic sea-level change across Anticosti Island (Québec, Canada). Geological Society of America Bulletin 123, 1645–1664.

Kah, L.C., Thompson, C.K., Henderson, M.A., Zhan, R., 2016. Behavior of marine sulfur in the Ordovician. Palaeogeography, Palaeoclimatology Palaeoecology 458, 133–153.

Kendall, B., Dahl, T.W., Anbar, A.D., 2017. The stable isotope geochemistry of molybdenum. Reviews in Mineralogy and Geochemistry 82, 683–732.

Kleinberg, A., Young, S.A., Owens, J.D., 2016. Geochemical investigation of environmental changes associated with the early Silurian Ireviken extinction event. Geological Society of America Abstracts with Programs 48, No. 7, https://doi.org/10.1130/abs/2016AM-286363.

Knoll, A.H., Carroll, S.B., 1999. Early animal evolution: Emerging views from comparative biology and geology. Science 284, 2129–2137.

Lenton, T.M., Crouch, M., Johnson, M., Pires, N., Dolan, L., 2012. First plants cooled the Ordovician. Nature Geoscience 5, 86–89.

Lenton, T.M., Dahl, T.W., Daines, S.J., Mills, B.J.W., Ozaki, K., Saltzman, M.R., Porada, P., 2016. Earliest land plants created modern levels of atmospheric oxygen. Proceedings of the National Academy of Sciences of the United States of America 113, 9704–9709.

Lenton, T.M., Daines, S.J., Mills, B.J.W., 2018. COPSE reloaded: an improved model of biogeochemical cycling over Phanerozoic time. Earth-Science Reviews 178, 1–28.

Ling, H., Chen, X., Li, D., Wang, D., Shields-Zhou, G.A., Zhu, M., 2013. Cerium anomaly variations in Ediacaran–earliest Cambrian carbonates from the Yangtze Gorges area, South China: implications for oxygenation of coeval shallow seawater. Precambrian Research 225, 110–127.

Lu, W., Ridgewell, A., Thomas, E., Hardisty, D.S., Luo, G., Algeo, T.J., Saltzman, M.R., Gill, B.C., Shen, Y., Ling, H.F., Edwards, C.T., Whalen, M.T., Zhou, X., Gutchess, K.M., Jin, L., Rickaby, R.E.M., Jenkyns, H.C., Lyons, T.W., Lenton, T.M., Kump, L.R., Lu, Z., 2018. Late inception of a resiliently oxygenated upper ocean. Science 361, 174–177.

Lu, Z., Jenkyns, H.C., Rickaby, R.E.M., 2010. Iodine to calcium ratios in marine carbonate as a paleo-redox proxy during oceanic anoxic events. Geology 38, 1107–1110.

Lyons, T.W., Severmann, S., 2006. A critical look at iron paleoredox proxies: New insights from modern euxinic marine basins. Geochimica et Cosmochimica Acta 70, 5698–5722.

Lyons, T.W., Anbar, A.D., Severmann, S., Scott, C., Gill, B.C., 2009. Tracking euxinia in the ancient ocean: a multiproxy perspective and Proterozoic case study. Annual Review of Earth and Planetary Sciences 37, 507–534.

Maloof, A.C., Schrag, D.P., Crowley, J.L., Bowring, S.A., 2005. An expanded record of Early Cambrian carbon cycling from the Anti-Atlas Margin, Morocco. Canadian Journal of Earth Science 42, 2195–2216.

Maloof, A.C., Ramezani, J., Bowring, S.A., Fike, D.A., Porter, S.M., Mazouad, M., 2010. Constraints on early Cambrian carbon cycling from the duration of the Nemakit-Daldynian-Tommotian boundary $\delta^{13}C$ shift, Morocco. Geology 38, 623–626.

Marenco, P.J., Marenco, K.N., Lubitz, R.L., Niu, D., 2013. Contrasting long-term global and short-term local redox proxies during the Great Ordovician Biodiversification Event: a case study from Fossil Mountain Utah, USA. Palaeogeography, Palaeoclimatology, Palaeoecology 377, 45–51.

Marenco, P.J., Martin, K.R., Marenco, K.N., Barber, D.C., 2016. Increasing global ocean oxygenation and the Ordovician Radiation: insights from Th/U of carbonates from the Ordovician of western Utah. Palaeogeography, Palaeoclimatology, Palaeoecology 458, 77–84.

Miller, A.I., Connolly, S.R., 2001. Substrate affinities of higher taxa and the Ordovician Radiation. Paleobiology 27, 768–778.

Mills, D.B., Ward, L.M., Jones, C., Sweeten, B., Forth, M., Treusch, A.H., Canfield, D.E., 2014. Oxygen requirements of the earliest animals. Proceedings of the National Academy of Sciences of the United States of America 111, 4168–4172.

Nursall, J.R., 1959. Oxygen as a prequisite to the origin of the metazoa. Nature 183, 1170–1172.

Ostrander, C.M., Owens, J.D., Nielsen, S.G., 2017. Constraining the rate of oceanic deoxygenation leading up to a Cretaceous Oceanic Anoxic Event (OAE-2: ~94 Ma). Science Advances 3, e1701020, http://dx.doi.org/10.1126/sciadv.1701020.

Owens, J.D., Gill, B.C., Jenkyns, H.C., Bates, S.M., Severmann, S., Kuypers, M.M.M., Woodfine, R.G., Lyons, T.W., 2013. Sulfur isotopes track the global extent and dynamics of euxinia during Cretaceous Oceanic Anoxic Event 2. Proceedings of the National Academy of Sciences of the United States of America 110, 18407–18412.

Owens, J.D., Reinhard, C.T., Rohrssen, M., Love, G.D., Lyons, T.W., 2016. Empirical links between trace metal cycling and marine microbial ecology during a large perturbation to Earth's carbon cycle. Earth and Planetary Science Letters 449, 407–417.

Owens, J.D., Lyons, T.W., Hardisty, D.S., Lowery, C.M., Lu, Z., Lee, B., Jenkyns, H.C., 2017. Patterns of local and global redox variability during the Cenomanian–Turonian Boundary Event (Oceanic Anoxic Event 2) recorded in carbonates and shales from central Italy. Sedimentology 64, 168–185.

Poulton, S.W., Fralick, P.W., Canfield, D.E., 2004. The transition to a sulphidic ocean, ~1.84 billion years ago. Science 431, 173–177.

Pruss, S.B., Finnegan, S., Fischer, W.W., Knoll, A.H., 2010. Carbonates in skeleton-poor seas: new insights from Cambrian and Ordovician strata of Laurentia. Palaios 25, 73–84.

Quinton, P.C., Herrmann, A.D., Leslie, S.A., Macleod, K.G., 2016. Carbon cycling across the southern margin of Laurentia during the Late Ordovician. Palaeogeography, Palaeoclimatology, Palaeoecology 458, 63–76.

Raff, R.A., Raff, E.C., 1970. Respiratory mechanisms and the metazoan fossil record. Nature 228, 1003–1005.

Raiswell, R., Hardisty, D.S., Lyons, T.W., Canfield, D.E., Owens, J.D., Planavsky, N.J., Poulton, S.W., Reinhard, C.T., 2018. The iron paleoredox proxies: a guide to the pitfalls, problems and proper practice. American Journal of Science 318, 491–526.

Reinhard, C.T., Planavsky, N.J., Robbins, L.J., Partin, C.A., Gill, B.C., Lalonde, S.V., Bekker, A., Konhauser, K.O., Lyons, T.W., 2013. Proterozoic ocean redox and biogeochemical stasis. Proceedings of the National Academy of Sciences of the United States of America 110, 5357–5362.

Royer, D.L., Donnadieu, Y., Park, J., Kowalczyk, J., Goddéris, Y., 2014. Error analysis of $CO_2$ and $O_2$ estimates from the long-term geochemical model GEOCARBSULF. American Journal of Science 314, 1259–1283.

Sahoo, S.K., Planavsky, N.J., Jiang, G., Kendall, B., Owens, J.D., Wang, X., Shi, X., Anbar, A.D., Lyons, T.W., 2016. Oceanic oxygenation events in the anoxic Ediacaran ocean. Geobiology 14, 457–468.

Saltzman, M.R., 2005. Phosphorus, nitrogen, and the redox evolution of the Paleozoic oceans. Geology 33, 573–576.

Saltzman, M.R., Young, S.A., 2005. Long-lived glaciation in the Late Ordovician? Isotopic and sequence-stratigraphic evidence from western Laurentia. Geology 33, 109–112.

Saltzman, M.R., Runnegar, B., Lohmann, K.C., 1998. Carbon isotope stratigraphy of upper Cambrian (Steptoean stage) sequences of the eastern Great Basin: record of a global oceanographic event. Geological Society of America Bulletin 110, 285–297.

Saltzman, M.R., Ripperdan, R.L., Brasier, M.D., Lohmann, K.C., Robison, R.A., Chang, W.T., Peng, S., Ergaliev, E.K., Runnegar, B., 2000. A global carbon isotope excursion (SPICE) during the Late Cambrian: relation to trilobite extinctions, organic-matter burial and sea level. Palaeogeography, Palaeoclimatology, Palaeoecology 162, 211–223.

Saltzman, M.R., Young, S.A., Kump, L.R., Gill, B.C., Lyons, T.W., Runnegar, B., 2011. Pulse of atmospheric oxygen during the late Cambrian. Proceedings of the National Academy of Sciences of the United States of America 108, 3876–3881.

Saltzman, M.R., Edwards, C.T., Leslie, S.A., Dwyer, G.S., Bauer, J.A., Repetski, J.E., Harris, A.G., Bergström, S.M., 2014. Calibration of a conodont apatite-based Ordovician $^{87}Sr/^{86}Sr$ curve to biostratigraphy and geochronology: implications for stratigraphic resolution. Geological Society of America Bulletin 126, 1551–1568.

Saltzman, M.R., Edwards, C.T., Adrain, J.M., Westrop, S.R., 2015. Persistent oceanic anoxia and elevated extinction rates separate the Cambrian and Ordovician radiations. Geology 43, 807–810.

Schiffbauer, J.D., Huntley, J.W., Fike, D.A., Jeffrey, M.J., Gregg, J.M., Shelton, K.L., 2017. Decoupling biogeochemical records, extinction, and environmental change during the Cambrian SPICE event. Science Advances 3, e1602158, http://dx.doi.org/10.1126/sciadv.1602158.

Schovsbo, N.H., 2002. Uranium enrichment shorewards in black shales: a case study from the Scandinavian Alum Shale. GFF 124, 107–116.

Sepkoski, J.J.J., 1998. Rates of speciation in the fossil record. Philosophical Transactions of the Royal Society of London B, Biological Sciences 353, 315–326.

Servais, T., Lehnert, O., Li, J., Mullins, G.L., Munnecke, A., Nützel, A., Vecoli, M., 2008. The Ordovician Biodiversification: revolution in the oceanic trophic chain. Lethaia 41, 99–109.

Servais, T., Owen, A.W., Harper, D.A.T., Kröger, B., Munnecke, A., 2010. The Great Ordovician Biodiversification Event (GOBE): the palaeoecological dimension. Palaeogeography, Palaeoclimatology, Palaeoecology 294, 99–119.

Sperling, E.A., Frieder, C.A., Raman, A.V., Girguis, P.R., Levin, L.A., Knoll, A.H., 2013. Oxygen, ecology, and the Cambrian radiation of animals. Proceedings of the National Academy of Sciences of the United States of America 110, 13446–13451.

Sperling, E.A., Knoll, A.H., Girguis, P.R., 2015a. The ecological physiology of Earth' s second oxygen revolution. Annual Review of Ecology, Evolution, and Systematics 46, 215–235.

Sperling, E.A., Wolock, C.J., Morgan, A.S., Gill, B.C., Kunzmann, M., Halverson, G.P., Macdonald, F.A., Knoll, A.H., Johnston, D.T., 2015b. Statistical analysis of iron geochemical data suggests limited late Proterozoic oxygenation. Nature 523, 451–454.

Swart, P.K., 2008. Global synchronous changes in the carbon isotopic composition of carbonate sediments unrelated to changes in the global carbon cycle. Proceedings of the National Academy of Sciences of the United States of America 105, 13741–13745.

Swart, P.K., Eberli, G., 2005. The nature of the $\delta^{13}C$ of periplatform sediments: implications for stratigraphy and the global carbon cycle. Sedimentary Geology 175, 115–129.

Terrell, F.M., 1973. Silicified trilobite zonation in the Lower Fillmore Formation in western Utah. Brigham Young University Geology Studies 20, 67–90.

Them, T.R., Gill, B.C., Caruthers, A.H., Gerhardt, A.M., Gröcke, D.R., Lyons, T.W., Marroquín, S.M., Nielsen, S.G., Trabucho-Alexandre, J.P., Owens, J.D., 2018. Thallium isotopes reveal protracted anoxia during the Toarcian (Early Jurassic) associated with volcanism, carbon burial, and mass extinction. Proceedings of the National Academy of Sciences of the United States of America 115, 6596–6601.

Thompson, C.K., Kah, L.C., 2012. Sulfur isotope evidence for widespread euxinia and a fluctuating oxycline in Early to Middle Ordovician greenhouse oceans. Palaeogeography, Palaeoclimatology, Palaeoecology 313–314, 189–214.

Tissot, L.H., Dauphas, N., 2015. Uranium isotopic compositions of the crust and ocean: age corrections, U budget and global extent of modern anoxia. Geochimica et Cosmochimica Acta 167, 113–143.

Towe, K.M., 1970. Oxygen-collagen priority and the early metazoan fossil record. Proceedings of the National Academy of Sciences of the United States of America 65, 781–788.

Trotter, J.A., Williams, I.S., Barnes, C.R., Lécuyer, C., Nicoll, R.S., 2008. Did cooling oceans trigger Ordovician biodiversification? Evidence from conodont thermometry. Science 321, 550–554.

Trubovitz, S., Stigall, A.L., 2016. Synchronous diversification of Laurentian and Baltic rhynchonelliform brachiopods: implications for regional versus global triggers of the Great Ordovician Biodiversification Event. Geology 44, 743–746.

Wallace, M.W., Shuster, A., Greig, A., Planavsky, N.J., Reed, C.P., 2017. Oxygenation history of the Neoproterozoic to early Phanerozoic and the rise of land plants. Earth and Planetary Science Letters 466, 12–19.

Weyer, S., Anbar, A.D., Gerdes, A., Gordon, G.W., Algeo, T.J., Boyle, E.A., 2008. Natural fractionation of $^{238}U/^{235}U$. Geochimica et Cosmochimica Acta 72, 345–359.

Wilson, M.A., Palmer, T.J., Guensburg, T.E., Palmer, W.M.A., Finton, C.D., Kaufman, L.E., 1992. The development of an Early Ordovician hardground community in response to rapid sea-floor calcite precipitation. Lethaia 25, 19–34.

Young, S.A., Saltzman, M.R., Bergström, S.M., Leslie, S.A., Xu, C., 2008. Paired $\delta^{13}C_{carb}$ and $\delta^{13}C_{org}$ records of Upper Ordovician (Sandbian–Katian) carbonates in North America and China: implications for paleoceanographic change. Palaeogeography, Palaeoclimatology, Palaeoecology 270, 166–178.

Young, S.A., Saltzman, M.R., Foland, K.A., Linder, J.S., Kump, L.R., 2009. A major drop in seawater $^{87}Sr/^{86}Sr$ during the Middle Ordovician (Darriwilian): links to volcanism and climate? Geology 37, 951–954.

Young, S.A., Saltzman, M.R., Ausich, W.I., Desrochers, A., Kaljo, D., 2010. Did changes in atmospheric $CO_2$ coincide with latest Ordovician glacial-interglacial cycles? Palaeogeography, Palaeoclimatology, Palaeoecology 296, 376–388.

Young, S.A., Gill, B.C., Edwards, C.T., Saltzman, M.R., Leslie, S.A., 2016. Middle–Late Ordovician (Darriwilian–Sandbian) decoupling of global sulfur and carbon cycles: isotopic evidence from eastern and southern Laurentia. Palaeogeography, Palaeoclimatology, Palaeoecology 458, 118–132.

Zhang, K., Zhu, X., Wood, R.A., Shi, Y., Gao, Z., Poulton, S.W., 2018. Oxygenation of the Mesoproterozoic ocean and the evolution of complex eukaryotes. Nature Geoscience 11, 345–350.

Zhou, X., Jenkyns, H.C., Owens, J.D., Junium, C.K., Zheng, X.Y., Sageman, B.B., Hardisty, D.S., Lyons, T.W., Ridgwell, A., Lu, Z., 2015. Upper ocean oxygenation dynamics from I/Ca ratios during the Cenomanian–Turonian OAE 2. Paleoceanography 30, 510–526.